Molecular Therapy
Original Article

Superagonist IL-15-Armed Oncolytic Virus Elicits Potent Antitumor Immunity and Therapy That Are Enhanced with PD-1 Blockade

Stacy J. Kowalsky,[1,2] Zuqiang Liu,[1,2] Mathilde Feist,[1,2,3] Sara E. Berkey,[1,2] Congrong Ma,[1,2] Roshni Ravindranathan,[1,2] Enyong Dai,[1,2] Edward J. Roy,[4] Zong Sheng Guo,[1,2] and David L. Bartlett[1,2]

[1]Department of Surgery, University of Pittsburgh School of Medicine, Pittsburgh, PA, USA; [2]UPMC Hillman Cancer Center, Pittsburgh, PA, USA; [3]Department of Surgery, CCM/CVK, Charité - Universitaetsmedizin Berlin, Berlin, Germany; [4]Department of Molecular and Integrative Physiology, University of Illinois at Urbana-Champaign, Urbana, IL, USA

Oncolytic immunotherapy is a promising novel therapeutic for cancer, and further preclinical studies may maximize its therapeutic efficacy. In this study, we construct a novel oncolytic vaccinia virus (VV) expressing a superagoinst IL-15, a fusion protein of IL-15 and IL-15Ralpha. This virus, named vvDD-IL15-Rα, possesses similar replication efficiency as the parental virus vvDD yet leads to significantly more regression of the disease and extends the survival of mice bearing MC38 colon or ID8 ovarian cancer. This novel virus elicits potent adaptive antitumor immunity as shown by ELISPOT assays for interferon-gamma-secreting $CD8^+$ T cells and by the rejection of tumor implants upon re-challenge in the mice, which were previously cured by vvDD-IL15-Rα treatment. *In vivo* cell depletion assays with antibodies showed that this antitumor activity is highly dependent on $CD8^+$ T cells but much less so on $CD4^+$ T cells and NK cells. Finally, the combination of the oncolytic immunotherapy with anti-PD-1 antibody dramatically improves the therapeutic outcome compared to either anti-PD-1 alone or vvDD-IL15-Rα alone. These results demonstrate that the IL-15-IL-15Rα fusion protein-expressing OV elicits potent antitumor immunity, and rational combination with PD-1 blockade leads to dramatic tumor regression and prolongs the survival of mice bearing colon or ovarian cancers.

INTRODUCTION

Cancer immunotherapy has made a breakthrough over the last 5 years. Yet, despite all the efforts in immunotherapy, only a minority of human patients benefit from these novel therapeutic regimens. Studies have shown that systemic potent antitumor immunity is required for significant efficacy of cancer immunotherapy.[1] However, the tumor microenvironment (TME) is highly immunosuppressive and limits both innate and adaptive antitumor immunity and promotes tumor growth.[2] In addition, the TME impacts the infiltration efficiency of tumor-specific T cells.[2,3]

Oncolytic virus (OV)-mediated cancer therapeutics are considered to be a novel type of immunotherapy.[4,5] The cancer cell death mediated by OVs is considered a form of immunogenic cell death (ICD).[5,6] This process of ICD provides multiple immune signals to activate the immune system. First, virally mediated cell death leads to the presentation of potent danger signals (signal 0) and tumor-associated antigens in context with major histocompatibility complex (MHC) class I antigens (signal 1) to dendritic cells (DCs) and other antigen-presenting cells. Then, viruses often induce inflammation and stimulate the production of cytokines and chemokines that activate and attract the immune cells into the TME (signals 3 and 4). These four signals, together with costimulatory signal (signal 2), elicit potent antitumor innate and adaptive immunity.[5–8] To enhance the potential efficacy of oncolytic therapy, investigators have designed various strategies to boost antitumor immunity, e.g., expressing genes to enhance tumor immunogenicity,[9,10] cytokines to stimulate antitumor immunity,[11–13] or in combination with other regimens of immunotherapy.[14–16]

Interleukin-15 (IL-15) is a cytokine capable of promoting survival, proliferation, and activation of natural killer (NK), NKT cells, and $CD8^+$ T cells,[17] as well as $CD56^+$ myeloid DCs.[18] In particular, IL-15 can potently and selectively stimulate memory $CD8^+$ T cells.[19,20] Despite the fact that it is a cytokine related to IL-2, it possesses contrasting roles in adaptive immune responses.[21] A number of studies indicate that IL-15 expressed in the TME may induce rejection of large tumors in a process mediated by T cells.[22] One unique property of IL-15 is that its bioactivity *in vivo* is conferred mainly through a *trans*-presentation mechanism, in which IL-15 is presented in complex with the α-subunit of soluble IL-15 receptor (IL-15R) to target cells such as NK, NKT, or T cells, rather than interact directly with membrane-bound IL-15R.[23,24] With this understanding, investigators have recently generated IL-15 agonists that consist of IL-15 and partial or complete soluble IL-15R to improve

Received 3 March 2018; accepted 12 July 2018;
https://doi.org/10.1016/j.ymthe.2018.07.013.

Correspondence: David L. Bartlett, MD, Department of Surgery, University of Pittsburgh School of Medicine, Pittsburgh, PA, USA.
E-mail: bartlettdl@upmc.edu
Correspondence: Z. Sheng Guo, PhD, Department of Surgery, University of Pittsburgh School of Medicine, Pittsburgh, PA, USA.
E-mail: guozs@upmc.edu

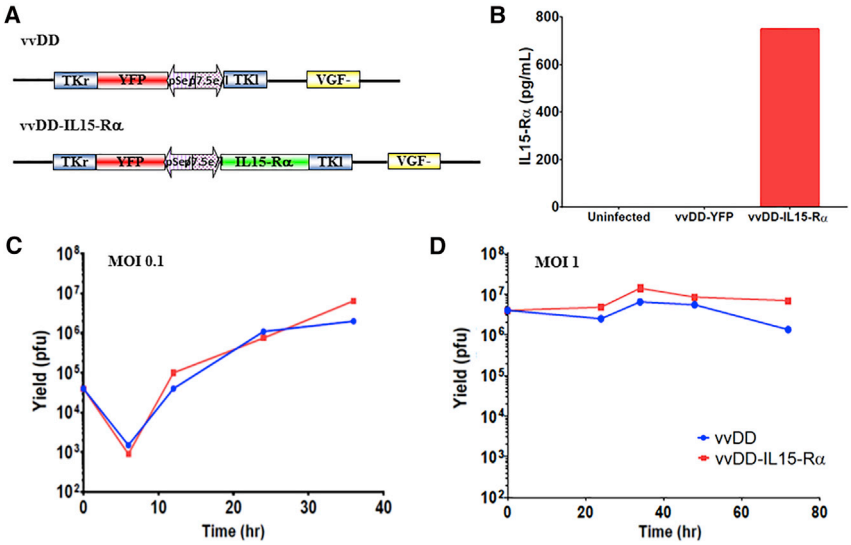

Figure 1. vvDD-IL15-Rα Replicates Similarly to vvDD and Produces the Fusion Cytokine *In Vitro*

(A) vvDD and vvDD-IL15-Rα viral constructs. TKr, the right portion of the *tk* gene; TKl, the left portion of the *tk* gene. (B) Production and secretion of IL-15 fusion protein from infected CV1 cells. Cells were mock-infected or infected with vvDD or vvDD-IL15-Rα at an MOI of 1.0 and conditioned media were harvested at 48 hr post-infection. The amount of the fusion protein secreted into the medium was quantified by an ELISA assay. (C and D) The yields of the two viruses in infected MC38-Luc cells. MC38-Luc cells were infected with vvDD or vvDD-IL15-Rα at MOIs of 0.1 or 1.0, then harvested at varying time points. Harvested cells were lysed, and the cell lysate was titered using viral plaque assay in CV1 cells. (C) MOI = 0.1, with assessment of viral replication at 6, 12, 24, and 36 hr after infection. (D) MOI = 1, with viral plaque assay performed on harvested cells at the same set of time points. This is representative of two experiments.

its *in vivo* bioactivity.[24,25] The soluble IL-15-IL-15Rα complexes greatly enhance IL-15 half-life and bioavailability *in vivo*, thus maximizing IL-15 activity.[23–28] Additional *in vivo* studies showed that this fusion protein can revive tumor-resident $CD8^+$ T cells and promote destruction of established tumors.[28] A study demonstrated that the IL-15 superagonist ALT-803 was superior to IL-15 for cancer immunotherapy in B16 melanoma and CT26 colon cancer models.[29] In addition, an IL-15 superagonist promotes not only immune responses of effector and memory $CD8^+$ T cells, but also antitumor activity of PD-1 blockade.[30] Investigators have explored the possibility of using an OV to express IL-15. Indeed, an IL-15-expressing oncolytic vesicular stomatitis virus has been shown to induce strong antitumor immunity in a murine colon cancer model.[31] An OV armed with both IL-15 and RANTES can enhance the function of CAR T cells.[32] Roy and associates[33] have shown that an oncolytic myxoma virus expressing this IL-15-IL-15Rα fusion protein possesses an enhanced antitumor activity in a B16 melanoma model.

We and others have been developing highly tumor-selective and potent oncolytic vaccinia viruses (VVs) for cancer virotherapy.[34] The virus vvDD contains two mutated viral genes encoding the thymidine kinase and vaccinia growth factor for improved the tumor selectivity.[35] This tumor-selective OV was proven to be safe in phase I clinical trials via either intratumoral injection or intravenous infusion. While some clinical responses were identified as a result of viral replication and oncolysis without a therapeutic transgene, an improvement in efficacy is still desired.[36,37] To enhance the therapeutic effect, our approaches include arming the virus with genes encoding chemokines, such as CXCL11,[11] and combining it with immune checkpoint blockade for synergistic efficacy.[15]

In this study, we have constructed an oncolytic VV encoding the murine fusion IL-15-IL-15Rα (vvDD-IL15-Rα). We hypothesized that oncolytic VV expressing bioactivity-enhanced IL-15-IL-15Rα complex could not only induce potent oncolytic effects with ICD, but also activate both T and NK cells and modulate the immune TME in favor of antitumor immunity. As a result, it would exhibit a superior antitumor activity and prolong the life of tumor-bearing mice. In this context, it is interesting to note that IL-15 and other common γ-chain-sharing cytokines (IL-2, IL-7, and IL-21) induce the expression of programmed death-1 (PD1) and its ligands (PD-L1).[38] Thus, the strategy of using PD-1 blockade in combination with this IL-15-armed OV might greatly improve the therapeutic outcome. Our current study has validated the hypothesis, and this new OV provides a superior therapeutic efficacy in both colorectal and ovarian cancer models.

RESULTS

Construction and *In Vitro* Characterization of the New Oncolytic VV vvDD-IL15-Rα

We constructed a new OV that expresses murine IL-15-IL-15Ra fusion gene in the backbone of a highly tumor-selective oncolytic VV vvDD. This new virus has been named vvDD-IL15-Rα (Figure 1A). First, we would verify the expression of the therapeutic gene IL-15 fusion protein. CV-1 cells were mock infected, infected with vvDD or vvDD-IL15-Rα at an MOI of 1.0, and conditioned media were harvested at 48 hr after infection. The quantity of IL-15-IL-15Ra fusion protein was determined by ELISA assay (Figure 1B). As we see, fusion protein reached 747 pg/mL in the media collected from vvDD-IL15-Rα-infected cells, while not detectable in medium from control vvDD-YFP-infected cells. Then we compared replication efficiency of this novel virus with a parental one in cancer cells. We infected MC38-Luc murine colon cancer cells with vvDD-IL15-Rα or parental virus vvDD at MOIs of 0.1 and 1 and then measured the replication efficiency by monitoring viral expansion over time using plaque assays. As shown in Figures 1C and 1D, the two viruses followed almost identical kinetics of progeny virus accumulation in MC38-Luc cancer cells. In addition, their oncolytic

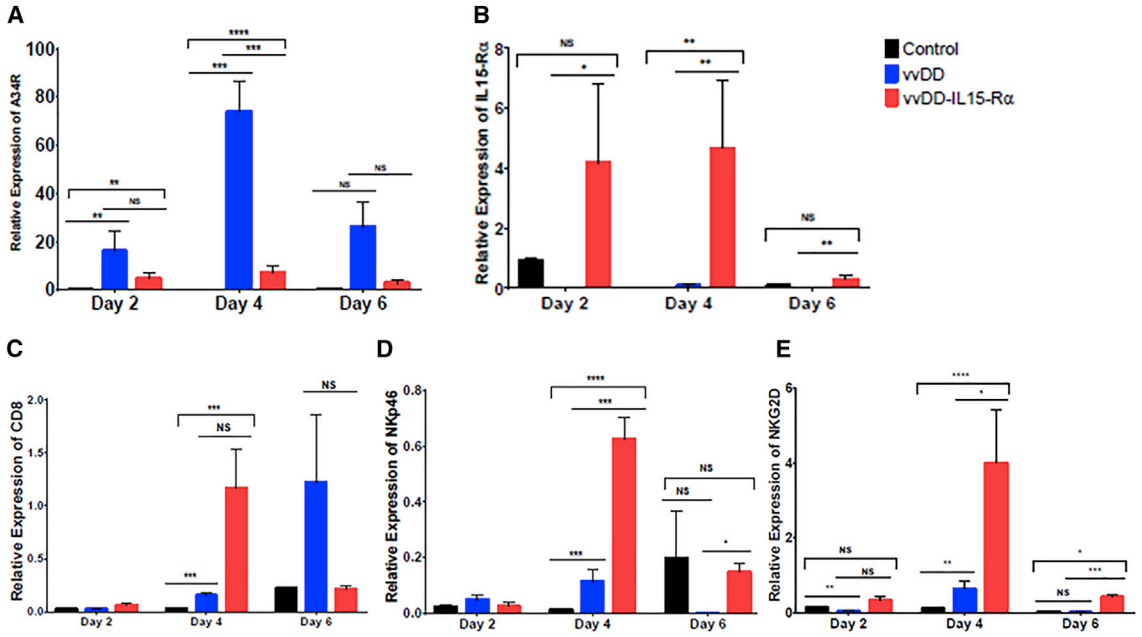

Figure 2. vvDD-IL15-Rα Replicates in MC38 Tumors, Expresses IL-15-IL-15Rα Fusion Protein, and Induces Immune Cell Infiltration to the Tumor Microenvironment

B6 mice were inoculated subcutaneously with 5.0e5 MC38-Luc cells on the right flank, then randomly divided into three groups (PBS, vvDD, and vvDD-IL15-Rα) once tumors reached 5 mm in diameter on caliper measurement. Mice were injected intravenously via tail-vein injection with PBS control or 1.0e8 PFU of vvDD or vvDD-IL15-Rα, and tumor tissue was harvested 2, 4, or 6 days later, after which total RNA was isolated from tumor homogenates and cDNA was created. The quantity of mRNA levels for relevant genes was then determined by qPCR analysis. (A) A34R, a marker of vaccinia virus accumulation, was expressed in tumor cells treated with vvDD and vvDD-IL15-Rα at all time points, indicating that the viruses infected and replicated within tumor tissue. (B) The IL-15-IL-15Rα fusion protein was expressed in tumors treated with vvDD-IL15-Rα. Expression of immune cell markers as an approximation of immune cell infiltration was assessed for (C) CD8 and (D and E) NK cell markers NKp46 (D) and NKG2D (E). All values presented as mean ± SEM. NS, not significant, *p < 0.05, **p < 0.01, ***p < 0.001, ****p < 0.0001.

potency in MC38 cancer cells was similar (Figure S1). In summary, these data demonstrated that inclusion of the fusion gene did not affect the functionality of the virus as a replicating OV and the viral construct appropriately secreted the fusion cytokine from infected cells *in vitro*.

vvDD-IL15-Rα Infects MC38 Colon Cancer Tissue, Expresses the Superagonist, and Induces Immune Cell Infiltration *In Vivo*

MC38-Luc tumors were established in C57BL/6 (B6) mice by injecting 5.0e5 MC38-Luc cells into the subcutaneous tissue of the right flank. Once tumors reached 5 mm in diameter, mice were treated intravenously with 1.0e8 plaque-forming units (PFU) of vvDD, vvDD-IL15-Rα, or just saline PBS. Tumor tissues were harvested 2, 4, and 6 days after treatment. Analysis by qRT-PCR of tumor homogenates showed viral infection of tumor tissues at all time points for vvDD and vvDD-IL15-Rα as evidenced by expression of A34R, a vaccinia coat protein gene (Figure 2A). Clearly, there was more accumulation of vvDD than vvDD-IL15-Rα ($p < 0.05$), suggesting that innate immunity activated by IL15-IL15Rα may facilitate the clearance of the virus. More importantly, the mRNA encoding the IL-15 fusion protein was expressed within tumor tissues of mice treated with vvDD-IL15-Rα at all examined time points (Figure 2B). These *in vivo* studies verified that both vvDD and vvDD-IL15-Rα were able to infect tumor implants *in vivo* and that the novel virus vvDD-IL15-Rα expressed the IL-15 fusion protein *in vivo*.

MC38-Luc tumor implants from mice treated with intravenous oncolytic VV were assessed for infiltration of immune cells after viral treatment with qPCR analysis. Both vvDD and vvDD-IL15-Rα induced expression of CD8 at day 4 and 6 after treatment, suggesting increased infiltration of $CD8^+$ T cells (Figure 2C). vvDD-IL15-Rα notably increased expression of activating NK cell receptors NKp46 (Figure 2D) and NKG2D (Figure 2E) at day 4 and day 6, suggesting increased activated NK cells in the TME.

vvDD-IL15-Rα Exhibits High Therapeutic Potency in Syngeneic MC38 Colon and ID8 Ovarian Cancer Models

We then tested the therapeutic potency of this new virus in murine tumor models. The peritoneal MC38 tumor model mimics a significant population of colorectal cancer patients with peritoneal metastases. 5.0e5 MC38-Luc cancer cells were injected into the peritoneal cavity of B6 mice (day 0). When the tumors were well established (day 5), randomized groups of mice were treated with PBS, vvDD, or vvDD-IL15-Rα at 2.0e8 PFU/mouse, intraperitoneally. Again, tumor growth was monitored by bioluminescence imaging, and animal health was closely monitored by observations

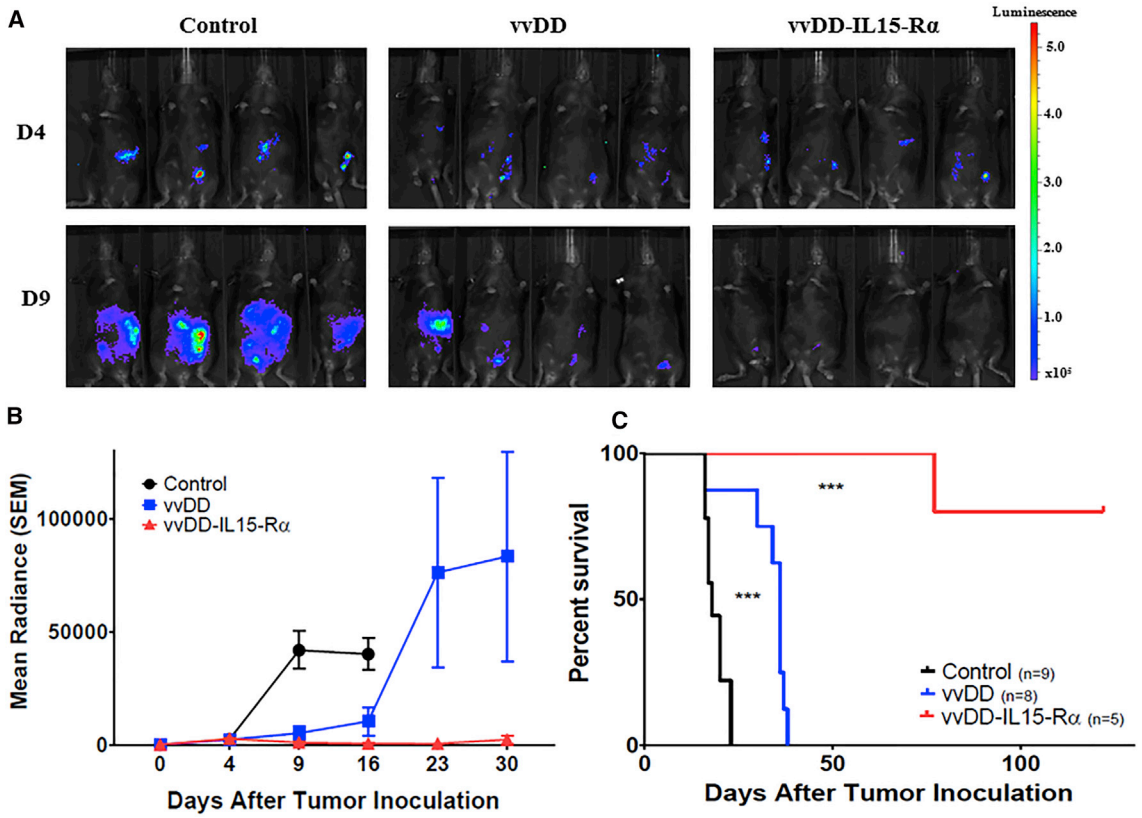

Figure 3. vvDD Expressing IL-15-IL15-Rα Delays Progression in MC38 Carcinomatosis and Significantly Improves Survival

B6 mice were inoculated i.p. with 5.0e5 MC38-Luc cells on day 0 (D0), then randomly divided into three groups (PBS, n = 9; vvDD, n = 8; and vvDD-IL15-Rα, n = 5) based on tumor burden via *in vivo* bioluminescent imaging on D4. On D5, mice were injected i.p. with 2.0e8 PFU of vvDD, vvDD-IL15-Rα, or PBS. (A) Representative intraperitoneal tumor burden in treatment groups at D4 (1 day prior to virus treatment) and D9 (4 days after virus treatment) via *in vivo* bioluminescent imaging. (B) Quantified data for tumor burden over experimental time course. Values are mean ± SD. (C) Animal survival of MC38-Luc tumor-bearing mice as Kaplan-Meier survival curves. More statistical analyses are presented in Table S1. ***$p < 0.001$.

and body weight measurements. Animal survival was recorded (Figure 3).

On day 4 (1 day before treatment), the tumor size, indicated by bioluminescence, was uniform in all groups. On day 9 (4 days after treatment), the mice in the control group had significant tumor mass on imaging. The parental virus vvDD displayed potent tumor growth inhibition; however, vvDD-IL-15Rα treatment resulted in a significant decrease in tumor mass (Figure 3A). vvDD initially inhibited tumor growth, yet tumor progressed at later time points (days 23 and 30). However, vvDD-IL15-Rα exhibited potent and long-term effects, with little tumor growth throughout 30 days of imaging (Figure 3B). When the animal survival was presented as a Kaplan-Meier survival curve, vvDD had a significant therapeutic effect, yet vvDD-IL15-Rα displayed far improved therapeutic effects, including 80% long-term cured mice (Figure 3C).

We performed a similar experiment with a syngeneic ID8 ovarian peritoneal cancer model (Figure 4). Three and a half million ID8-luc cells were injected into B6 mice, and tumor growth was monitored by bioluminescent imaging. On day 11, three randomized groups of mice were treated with PBS, vvDD, or vvDD-IL15-Rα. As demonstrated in Figure 4A, vvDD treatment resulted in significant growth inhibition, and vvDD-IL15-Rα treatment significantly decreased tumor mass compared to vvDD on day 25. In Figure 4B, it is apparent that vvDD inhibited tumor growth compared to control, but vvDD-IL15-Rα significantly reduced tumor mass compared to vvDD. The Kaplan-Meier survival curve demonstrates a similar pattern of potencies for the two OVs in this ovarian cancer model as observed in the previous colon cancer model (Figure 4C). Overall from both tumor models, it is clear that vvDD-IL15-Rα demonstrates marked anti-cancer therapeutic efficacy.

vvDD-IL15-Rα Induces Potent Adaptive Anti-tumor Immunity

After demonstrating potent antitumor efficacy of this novel virus, we explored the mechanisms of action. First, we assessed the number of $CD8^+$ T cells and their anti-tumor activity, collected from peritoneal cavity lavage 10 days after viral treatment (Figure 5). We observed that about 10% of the total i.p. cells were $CD8^+$ T cells in the PBS-treated mice. However, in mice treated with either virus, the

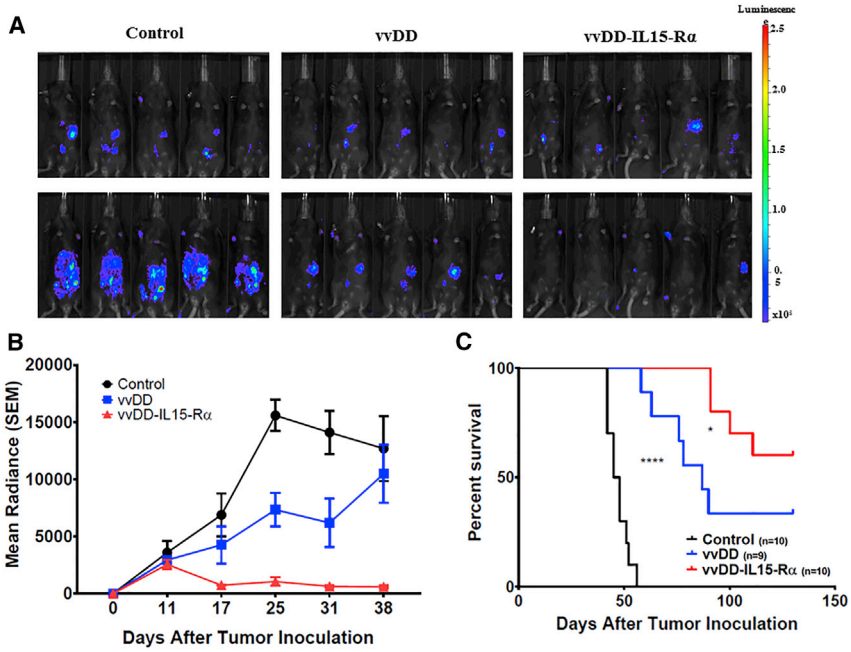

Figure 4. vvDD-IL15-Rα Induces Regression of ID8-luc Ovarian Carcinomatosis and Improves Survival over vvDD Alone

B6 were injected i.p. with 3.5e6 ID8-Luc cells on day 0 (D0). Mice were then randomized into control (n = 10), vvDD (n = 9), and vvDD-IL15-Rα (n = 10) groups based on tumor burden assessed by *in vivo* bioluminescent imaging on D11, after which mice were treated i.p. with 2.0e8 PFU vvDD, vvDD-IL15-Rα, or PBS. (A) Representative intraperitoneal tumor burden in treatment groups at D11 (prior to viral treatment) and D25 (14 days after virus treatment) via *in vivo* bioluminescent imaging. (B) Quantified group radiance over experimental course, representing tumor burden assessed with *in vivo* bioluminescent imaging. Values are mean ± SD. (C) Animal survival of ID8-Luc tumor-bearing mice as Kaplan-Meier survival curves (Table S1). *p < 0.05, ****p < 0.0001.

percentage significantly increased to about 30% (Figure 5A). This may indicate that the inflammation caused by the virus results in a significant infiltration of $CD8^+$ T cells into tumor tissue and vicinity. We examined the anti-tumor activity of these $CD8^+$ T cells by interferon (IFN)-γ-ELISPOT assay, in the presence or absence of irradiated MC38-Luc cells (Figure 5B). The $CD8^+$ T cells harvested from PBS control group showed very few IFN-γ^+ spots, indicating few tumor-specific activated $CD8^+$ T cells. The vvDD virus-treated mice did show increased yet very limited numbers of IFN-γ^+ spots. On the other hand, vvDD-IL15-Rα-treated mice showed a dramatically enhanced number of IFN-γ^+ spots, indicating significantly more tumor-specific activated $CD8^+$ T cells (Figures 5B and 5C). The vvDD-IL15-Rα-treated mice which had been cured with a single treatment (n = 4) were re-challenged with parental MC38-Luc cells. The mice were completely resistant to re-challenge (Figure 5D). These results demonstrate that this superagonist protein in the context of an OV potently stimulates anti-tumor adaptive immunity.

To determine which major types of immune cells are needed for the virus-induced anti-tumor activity, we then repeated the murine experiments by depleting NK, $CD4^+$, and $CD8^+$ cells using antibodies (Figure 5E). The dosing and timing of the antibody administration were done under the conditions where the efficiency of cell depletion reached in previous studies.[15] In addition, we have done monitoring of efficacy of cell depletion in small groups of mice to show the depletions of immune cell types worked in the current study. For example, we showed that $CD3^+CD8^+$ T cells had been reduced 80%–90% at 27 days post-first-injection of the anti-murine CD8 antibody.

Under these conditions, tumors rapidly progressed as expected in control-treated mice, while mice treated with vvDD-IL-15Rα had delayed progression. When $CD8^+$ cells were depleted in the mice treated with the OV, tumors progressed more rapidly, especially when compared to mice with depletion of NK and $CD4^+$ T cells (Figure 5F). Correspondingly, the control mice had a median survival of 18 days, while the mice treated with vvDD-IL15-Rα all had a significant survival benefit. The depletion of $CD8^+$ cells led to significantly reduced survival compared to other viral treatments (median survival 47 days), however, the depletion of either $CD4^+$ cells or NK cells had minimal effects, with median survival greater than 150 days (data not shown). These results demonstrated that $CD8^+$ T cells play a critical role for the therapeutic efficacy mediated by this IL-15 superagonist-expressing OV.

Rational Combination of the OV with PD-1 Blockade Dramatically Improved the Therapeutic Efficacy

During the molecular analysis of tumor immune microenvironment, we found that PD-1s in the tumor tissue were significantly increased on days 4 and 6 after treatment with vvDD-IL15-Rα (Figure 6A; Figure S2A). It is interesting to note that PD-L1 was also significantly upregulated on day 2 (Figure S2B). In our previous study, we found that the combination of vvDD with PD-L1 blockade could work synergistically to improve therapeutic efficacy in both MC38 colon and ID8 ovarian cancer models.[15] Here, we chose to explore whether the improved results with vvDD-IL15-Rα could be further enhanced with anti-PD1 therapy in MC38 tumor model. Again, both OVs had significant therapeutic effects, with greater results from vvDD-IL15-Rα (Figure 6B). The treatment with anti-PD-1 antibody also improved survival, and combination of vvDD with anti-PD-1 further improved the anti-tumor efficacy. When all groups are plotted together, the combination of vvDD-IL15-Rα plus anti-PD-1 antibody had the most dramatic effect, extending the survival of mice to over 200 days ($p \leq 0.001$ compared to any other group). This results showed greatly improved survival when compared to the combination of vvDD-CXCL11 and anti-PD-L1 antibody used in the tumor model in our previous study.[15] In summary, the combination of

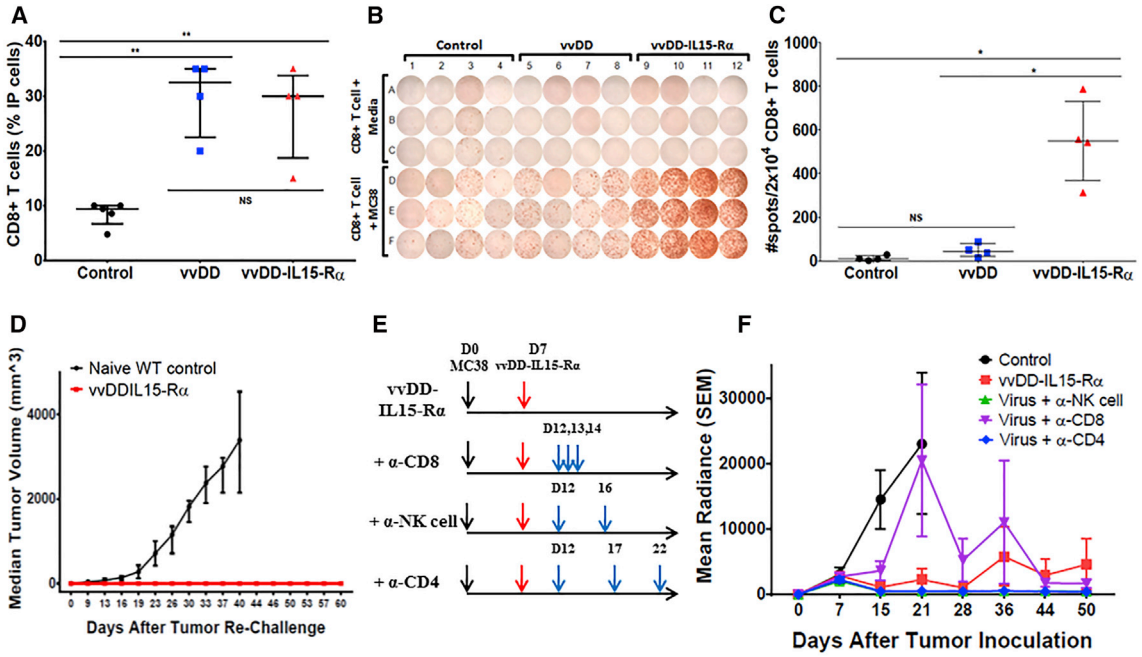

Figure 5. vvDD-IL15-Rα Stimulates CD8⁺ T Cell-Dependent Anti-tumor Immunity and Generates Immune Memory against Cancer Cells

Peritoneal MC38 tumor-bearing mice were randomized and injected i.p. with 2.0e8 PFU of vvDD (n = 8), vvDD-IL15-Rα (n = 7), or PBS (n = 5) 9 days after tumor inoculation. On day 19 (D19), i.p. lavage was performed, with virus-treated mice grouped in pairs. $CD8^+$ T cells were isolated from single-cell i.p. suspensions (2.0e7) by antibody bead column separation. (A) vvDD and vvDD-IL15-Rα induced significant increases in infiltrating $CD8^+$ T lymphocytes (TILs) to the TME compared to PBS. 2.0e4 TILs were incubated with 2.0e4 irradiated MC38-Luc cells for 24 hr, then IFN-γ ELISPOT analysis was performed to detect tumor-reactive TILs. (B) vvDD-IL15-Rα significantly induced formation of MC38-reactive TILs. (C) Graphical representation of MC38-reactive TILs from peritoneal lavage. B6 mice were inoculated i.p. with 5.0e5 MC38-Luc cancer cells and grouped into five groups (n = 10) based on tumor burden via *in vivo* bioluminescent imaging. PBS or 2e8 PFU vvDD-IL15-Rα was injected i.p. on day 7 (D7). (D) MC38-Luc tumor-bearing mice with tumor regression after intraperitoneal vvDD-IL15-Rα (at 2.0e8 PFU) treatment (132 days after initial tumor inoculation; shown in Figure 3C; n = 4) and naive B6 mice (n = 8) were injected subcutaneously in the right flank with 1.0e6 MC38-Luc cancer cells. Tumor growth was monitored over time using electric calipers to measure tumor size in two dimensions. B6 mice bearing i.p. MC38-Luc tumors were injected i.p. with PBS or 2.0e8 PFU vvDD-IL15-Rα on day 7 (D7) following assessment of tumor burden with *in vivo* bioluminescent imaging. (E) Antibody immune cell depletion was then performed individually for $CD8^+$ T cells (250 μg), NK cells (α-Asialo GM1, 50 μL/each mouse; Wako Chemicals), and $CD4^+$ T cells (150 μg) via i.p. injection following the depicted schedule. (F) Quantified group radiance over experimental course, representing tumor burden assessed with *in vivo* bioluminescent imaging shows accelerated tumor progression in mice treated with vvDD-IL15-Rα when $CD8^+$ T cells were depleted (Table S1). Values are mean ± SD. Data are representatives of 2–3 independent experiments. NS, not significant, *$p < 0.05$, **$p < 0.01$.

vvDD-IL15-Rα and anti-PD1 dramatically improved the therapeutic efficacy and survival of the mice bearing MC38 colon tumor.

DISCUSSION

The IL-15 superagonist, a fusion protein of IL-15 and IL-15Rα, has been previously shown to be superior to IL-15 in promoting adaptive antitumor immunity. Our highly tumor-selective OV, vvDD, has undergone two clinical trials and proved to possess a high safety profile, with some evidence of therapeutic efficacy in a subgroup of human cancer patients.[36,37] To further improve its efficacy, we incorporated this IL-15-IL-15Rα fusion gene into vvDD, hoping to achieve the best combination of two classes of therapeutic agents. We have confirmed that this armed OV expressed the fusion protein from the virus-infected cells by ELISA assay and then in MC38 tumor tissues by RT-PCR.

We then moved to test its gene expression kinetics, potential safety, and efficacy in colon and ovarian tumor models in syngeneic mice. We first examined the expression kinetics of the superagonist by qRT-PCR. In this model of MC38 colon cancer, the expression of IL-15 fusion protein (or mRNA) peaked on day 4 and declined to low levels by day 6. We observed increased expression of markers for NK and T cells, suggesting superagonist IL-15 functions to enhance the infiltration and/or activation of NK and T cells in the tumor tissues, when compared to the parental virus vvDD. The kinetics of the inflammatory response between vvDD-IL15-Rα and vvDD seem to be different. vvDD-IL15-Rα induces CD8 T cells rapidly, leading to rapid clearance of the virus and tumor cells. The parental virus (vvDD) activates the immune system with slower kinetics, probably reaching a plateau by day 6.

Then we examined the efficacy of the armed OV. In the intraperitoneal (i.p.) model of MC38 colon cancer, vvDD-IL15-Rα exhibited more potent antitumor activity and thus displayed better survival of mice initially bearing MC38-Luc tumors. Similar pattern of antitumor activity was also observed in ID8-Luc ovarian cancer in syngeneic

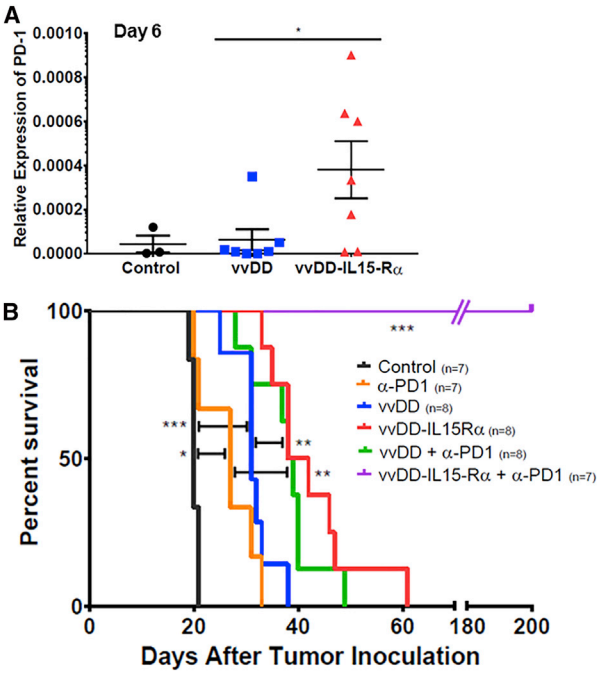

Figure 6. vvDD-IL15-Rα Induces PD-1 Expression in the MC38 Tumor Microenvironment and PD-1 Blockade Dramatically Improves vvDD-IL15-Rα Anti-tumor Efficacy

(A) PD1 expression in subcutaneous MC38 tumors. B6 mice were inoculated subcutaneously with 5.0e5 MC38-Luc cells on the right flank, then randomly divided into three groups (PBS, vvDD, and vvDD-IL15-Rα) once tumors reached 5 mm in diameter on caliper measurement. Mice with injected intravenously via tail-vein injection with PBS control or 1.0e8 PFU of vvDD or vvDD-IL15-Rα and tumor tissue was harvested 2, 4, and 6 days later, total RNA was isolated from tumor homogenates, and cDNA was created for qPCR analysis. PD1 expression on days 6 (and 4) was significantly increased in the tumor microenvironment of tumors treated with vvDD-IL15-Rα. Values represent mean ± SD. (B) Survival experiment with MC38 i.p. tumor model. B6 mice were inoculated i.p. with 5.0e5 MC38-Luc cells, then divided into random groups on day 7 (D7) based on tumor burden on *in vivo* bioluminescent imaging. Mice were then treated i.p. with 2.0e8 PFU of vvDD, vvDD-IL15-Rα, or PBS control on D7, with or without 200 μg of anti-PD-1 Ab, which was given every 2 days for a total of four doses. Survival of MC38-Luc tumor-bearing mice treated with PBS, vvDD, or vvDD-IL15-Rα with or without PD-1 blockade as Kaplan-Meier survival curves shows 100% survival of mice treated with vvDD-IL15-Rα + PD-1 blockade (Table S1). Data are representative of two independent experiments. *$p < 0.05$, **$p < 0.01$, and ***$p < 0.001$.

mice. Our study strongly suggests that IL-15 superagonist and OV together elicited highly potent antitumor $CD8^+$ T cells, as shown by ELISPOT assay and parental tumor cell re-challenge (MC38 tumor) in the cured mice. Cell depletion experiments demonstrated that $CD8^+$ T cells, but not $CD4^+$ T cells or NK cells, are important in mediating antitumor activity under these conditions. In summary, this superagonist IL-15-expressing OV acts through $CD8^+$ T cell-dependent adaptive antitumor immunity.

It is intriguing that this antitumor activity was independent of NK cells as one of the major functions of IL-15 is to activate NK cells in addition to T cells. There are several explanations for the result. One is that the timing of anti-Asialo GM1 antibody treatment (5 and 9 days after viral treatment) may not have been appropriate to have an effect on the rapidly activated NK cells that function with an early kinetics. The other possibility is that VV can inhibit NK cell functions in the TME through direct infection.[39] The third possibility is that the virus encodes multiple genes whose products are to inhibit NK cells as well as other immune cells via inhibition of the nuclear factor κB (NF-κB) pathway.[40] In this regard, it is tempting to explore the removal of these NF-κB inhibitors from this OV, as it may greatly enhance the therapeutic response.[41]

OVs have demonstrated promising results in the treatment of cancer as showcased by the FDA approval of first-in-class drug talimogene laherparepvec (T-VEC). The combinatorial strategy for cancer therapy has been a well-recognized consensus for highly efficacious means among leading investigators. We and others have explored the combination of virotherapy with immune checkpoint blockade.[42,43] In our previous study, we showed that the viral infection of cancer tissue caused inflammation and induction of PD-L1 and possibly PD1, and thus it was logical to combine an OV and anti-PD-L1 antibody for synergistic therapeutic effects in multiple tumor models.[15] It has been shown that PD1 and PD-L1 could be induced by IL-15 and other common γ-chain-sharing cytokines.[38] Indeed, we showed here that after treatment with vvDD-IL15-Rα, PD-1, and PD-L1 as well were upregulated in tumor tissues. It is not clear which cell types in the TME account for the increase in PD-L1, and further studies delineating the origin may be indicated. IL-15 is known to increase PD-L1 on T cells,[38] and this may account for the differences noted. When this OV was combined with anti-PD-1 blockade, we observed our most striking therapeutic efficacy ever, with all tested mice surviving for the duration of the experiment, over 200 days (Figure 6). To the best of our knowledge, this is the best therapeutic efficacy in this syngeneic tumor model among any treatment strategies.

One rationale for the combination with immune checkpoint blockade is that an OV often induces inflammation and upregulates PD-1 and/or PD-L1 in the tumor tissues.[15] It is interesting to note this combination has been tested in human cancer patients, with two clinical studies combining an OV (GM-CSF-armed oncolytic herpes simplex virus) and one of the immune checkpoint blockers.[44,45] In the first, a phase Ib study in patients with metastatic melanoma, the authors reported that the injection of T-VEC intratumorally in combination with systemic anti-PD-1 treatment resulted in enhanced T cell infiltration in the OV-injected tumor lesions and 62% response rate.[44] In the second, randomized, open-label phase II study, ipilimumab, an anti-CTLA4 antibody, was used alone or in combination with T-VEC to treat advanced melanoma patients. The results showed that 39% in the combination arm and 18% in the ipilimumab alone arm had an objective response. Interestingly, responses were not limited to injected lesions.[45] These studies demonstrate that the combination regimens are better than monotherapy in achieving higher objective responses in melanoma patients.

In summary, our current study has revealed that an OV armed with an activity enhanced superagonist IL-15 can elicit potent adaptive antitumor immunity and significant antitumor activity in two tumor models in mice, and the combination of this OV with anti-PD1 blockade exhibits striking therapeutic efficacy in a murine colon cancer model. While this data is based on a murine version of IL-15-IL-15Rα, the homologous human version can be substituted for easy translation into patients. Our results warrant clinical applications with such combination regimen of vvDD-IL-15Rα in cancer patients.

MATERIALS AND METHODS

Mice and Cell Lines

Female C57BL/6J mice (B6) were purchased from the Jackson Laboratory (Bar Harbor, ME) and were housed in the University of Pittsburgh animal facility under pathogen-free conditions. The Institutional Animal Care and Use Committee approved all animal studies and procedures performed. A murine colon cancer cell line transduced with a lentivirus expressing firefly luciferase gene, MC38-Luc, was previously used in the laboratory,[46] and murine ovarian cancer cells labeled with firefly luciferase, ID8-Luc, were obtained from Dr. Natasa Obermajer (University of Pittsburgh).[47] HeLa and CV-1 cells, for viral amplification and titering, were originally obtained from ATCC (Manassas, VA). All cells were grown in DMEM supplemented with 1× penicillin and streptomycin (Invitrogen, Carlsbad, CA), 2 mM L-glutamine, and 10% fetal bovine serum (FBS) in an incubator at 37°C with 5% CO_2.

Generation of vvDD-IL15-Rα

The DNA fragment containing murine IL-15Ra sushi domain-IL-15 fusion gene was amplified via PCR from plasmid pBS-IL-15RLI-tdTomato,[33] using primer set SalI-Sushi forward primer 5′-TAC GTCGACTATAAATAGATGGAGACAGACACACT-3′ and AscI-mIL-15 reverse primer 5′-TAGGCGCGCCTTATCAGCTGGTGTT GATGAACATC-3′.

Then the restriction enzyme (SalI and AscI)-digested DNA fragment was cloned into the respected sites in pCMS-IRES, a derivative of pCMS1 plasmid.[48] This results in a new shuttle vector, pCMS-IL15-Rα. To construct the new virus, called vvDD-IL15-Ra, vSC20, a Western Reserve (WR) strain VV with a deletion in *vgf*, was used as a parental virus to infect CV-1 cells (~2.0e5 cells) in 6-well plate at an MOI of 0.1 for 2 hr before the shuttle plasmid pCMS-IL15-Rα (2 μg) was transfected into these CV-1 cells. Two to three days later, the new virus was selected based on expression of YFP using multiple rounds of flow sorting and plaque purification, as described.[49] A recombinant VV with the same genetic deletions for two viral genes (vvDD or vvDD-YFP) was used as a control in the study.

Viral Replication *In Vitro*

In vitro viral replication assays comparing vvDD and vvDD-IL15-Rα were performed as previously described.[46] 1.0e5 MC38-Luc were plated on 6-well plates and incubated overnight. The MC38-Luc cells were then infected with vvDD or vvDD-IL15-Rα at MOIs of 0.1 and 1 in 1 mL of 2% FBS-containing DMEM media for 2 hr. The cells infected with virus at MOI 0.1 were then harvested 6, 12, 24, and 36 hr later, while the cells infected with virus at MOI 1 were harvested after 24, 36, 48, and 72 hr. Following harvest, the cell pellets were homogenized to release intracellular virions using Precellys 24 Tissue Homogenizer (Bertin Instruments, Rockville, MD). The viral load of cell lysates was then determined by viral plaque assay in CV-1 cells.

Murine Tumor Models

Initially, subcutaneous MC38 tumor in syngeneic C57BL/6J (B6 in short) mice was used for some studies. This was done by injecting 5.0e5 MC38 tumor cells into the right flank of mice. For peritoneal carcinomatosis models, B6 mice were injected intraperitoneally with 5.0e5 MC38-Luc or 3.5e6 ID8-luc cells, and 5 and 11 days later, respectively, mice were randomly divided into three groups based on tumor growth via *in vivo* bioluminescent animal imaging, using Xenogen IVIS Optical *In Vivo* Imaging System (Caliper Life Sciences, Hopkinton, MA). The groups of mice were then injected intraperitoneally with vvDD or vvDD-IL15-Rα at 2.0e8 PFU/200 μL or 200 μL PBS as control. Mice with inadvertent subcutaneous tumor cell inoculation were excluded from analysis given that tumors extended beyond the peritoneal cavity. In an additional experiment, rat-anti-mouse monoclonal antibodies (Ab) were used to selectively deplete certain types of immune cells in the following manner: anti-mouse anti-asialo GM1 Ab at 50 μL/injection per instruction from the supplier (Wako Chemicals USA, Richmond, VA), anti-mouse CD8 Ab at 250 μg/injection (clone 53-6.7, BioXCell, West Lebanon, NH), and anti-mouse CD4 Ab at 150 μg/injection (clone GK1.5, BioXCell) for depletion of NK, $CD8^+$ T cells, and $CD4^+$ T cells, respectively. Additionally, rat-anti-mouse monoclonal anti-PD-1 Ab (clone RMP1-14, BioXCell) was utilized to inhibit PD-1/PD-L1 interaction and was injected intraperitoneally (200 μg/injection) every other day for four doses total.

Long-term survivors of intraperitoneal MC38 tumor inoculation and vvDD-IL15-Rα treatment were re-challenged with MC38-Luc tumor implants (1.0e6 cells/mouse) injected subcutaneously on the right flank 132 days after initial intraperitoneal tumor inoculation. Tumor growth was monitored via digital caliper volume measurement and compared to naive B6 mice inoculated with MC38-Luc tumor implants at the same time. Tumor volume was calculated as: V_{tumor} (mm^3) = 0.5 (L × W2).

Live Animal Bioluminescence Imaging

Implanted tumor cells were originally transduced with lentivirus expressing firefly luciferase, allowing for *in vivo* live animal bioluminescence imaging with a Xenogen IVIS 200 Optical *In Vivo* Imaging System (Caliper Life Sciences, Hopkinton, MA), using well-established standard procedures.[50] In brief, mice were injected peritoneally with 0.1 mL of 0.1 M D-luciferin, potassium salt (GoldBio, St Louis, MO), for 5–10 min before they were anesthetized and aligned in the compartment of the instrument for bioluminescence imaging (BLI). BLI was performed prior to virus or mock treatments to ensure that tumor implants were present and that groups had comparable

tumor burden. IVIS live animal BLI was then performed periodically following treatment to monitor tumor progression.

Assessment of Animal Health and Survival

Animal health status and survival was monitored closely. Abdominal girth of mice bearing intraperitoneal tumor implants was monitored with caliper measurement, and mice were sacrificed when girth exceeded 1.5× original measurements. Mice either succumbed to their disease or were sacrificed when abdominal girth exceeded allowable measurements as above. Mice with subcutaneous tumor implants were sacrificed when tumors reached maximum diameter of 2 cm, became ulcerated, and/or interfered with murine activity.

TME Analysis

B6 mice were injected with 5.0e5 MC38-Luc tumor cells subcutaneously on the right flank to establish tumor implants. Once tumor implants reached 5 mm in diameter, mice were treated intravenously with 1.0e8 PFU of vvDD, vvDD-IL15-Rα, or PBS administered via tail-vein injection. Tumor tissues were recovered 2, 4, and 6 days after virus or mock treatment and then homogenized using Precellys 24 Tissue Homogenizer (Bertin Instruments, Rockville, MD).

RT-qPCR

RNA was isolated from tumor homogenates of subcutaneous MC38-Luc tumor implants using RNeasy kit (QIAGEN, Germantown, MD). cDNA was then created using from 2 μg of RNA using qScript cDNA SuperMix (Quanta Biosciences, Gaithersburg, MD) and Dyad Peltier Thermal Cycler (Bio-Rad, Hercules, CA). qPCR was then performed using TaqMan analysis with PerfeCTa qPCR SuperMix (Quanta Biosciences) on the StepOnePlus System (Life Technologies, Grand Island, NY). All PCR primers were purchased from Thermo Fisher Scientific (Waltham, MA) and are listed in Table S2. A novel set of primers and hybridization oligomer for the codon-optimized IL-15-IL-15Rα was created for qPCR: forward primer, 5′-TGAGGAAC GTGCTGTACCTG-3′; reverse primer, 5′-GGTCTTCTCCTCC AGCTCCT-3′; and hybridization oligomer, 5′-GAGAGCGGCTGT AAGGAGTG-3′. This will produce a product of 98 base pairs. Relative gene expression was compared to a housekeeping gene, either hypoxanthine-guanine phosphoribosyltransferase (HPRT1) or glyceraldehyde 3-phosphate dehydrogenase (GAPDH) and was expressed as fold increase ($2^{-\Delta CT}$), where $\Delta CT = CT_{(\text{target gene})} - CT_{(\text{HPRT1 or GAPDH})}$.

ELISA Assay for Murine IL15-Rα Protein

The concentration of IL15-Rα fusion protein in the supernatants of cancer cell culture was quantified using mouse IL-15 DuoSet ELISA kit according to the manufacturer's instructions (R&D Systems, Minneapolis, MN).

IFN-γ ELISPOT Assay

Intraperitoneal MC38-Luc tumor bearing mice were treated intraperitoneally with 2.0e8 PFU virus of either vvDD or vvDD-IL15-Rα, or PBS at day 9 after tumor inoculation. Ten days after virus or mock treatment, intraperitoneal lavage was performed during which an 18G needle was used to inject 5 mL of 2% FBS-PBS into the peritoneal cavity, and then the cavity was gently agitated before the volume was aspirated and repeated one to two times. Lavage volume was strained over a 100 μM cell strainer, and red blood cells were lysed using ACK Lysing Buffer (Thermo Fisher Scientific, Waltham, MA) prior to final straining over a 40 μM cell strainer. Isolation of $CD8^+$ T cells from 2.0e7 i.p. cells was then performed using α-mouse CD8 microbead isolation protocol (Miltenl Biotec, San Diego, CA). Once isolated, 2.0e4 $CD8^+$ T cells were stimulated with 4,000-rad-irradiated MC38 cells (2.0e4) in RPMI 1640 media supplemented with 10% FBS at 37°C, 5% CO_2 for 24 hr. Following incubation, plates were appropriately washed before incubation with biotinylated α-mouse IFN-γ (monoclonal antibody [mAb] R4-GA2-Biotin, Mabtech, Cincinnati, OH). After 36 hr of incubation, ELISPOT plates were then developed according to vendor protocols for Vectastain Elite ABC and AEC Peroxidase substrate (SK-4200) kits (Vector Laboratories, Burlingame, CA). Plates were read and analyzed using an ImmunoSpot analyzer (Cellular Technology, Shaker Heights, OH).

Statistical Analysis

GraphPad Prism version 7 (GraphPad Software, San Diego, CA) was used in creating graphs and analyzing data from both *in vitro* and *in vivo* studies. The data analysis was performed using non-parametric Student's t test or two-way ANOVA. Survival of animals was assessed using Kaplan-Meier survival curves and was analyzed using log rank (Mantel-Cox) test. A p value of < 0.05 was considered statistically significant. The symbols used in figures were standard ones: *$p < 0.05$; **$p < 0.01$; ***$p < 0.001$; ****$p < 0.0001$; and NS, not significant.

SUPPLEMENTAL INFORMATION

Supplemental Information includes two figures and two tables and can be found with this article online at https://doi.org/10.1016/j.ymthe.2018.07.013.

AUTHOR CONTRIBUTIONS

S.J.K., Z.S.G., and D.L.B. conceived and designed the experiments and interpreted the data. S.J.K., Z.L., M.F., S.E.B., C.M., R.R., and E.D. performed the experiments. E.J.R. provided essential reagents. S.J.K., Z.S.G., and D.L.B. wrote the paper.

CONFLICTS OF INTEREST

D.L.B. has financial interests with SillaJen Biotherapeutics. The other authors declare no conflict of interest.

ACKNOWLEDGMENTS

This work was supported in part by David C. Koch Regional Cancer Therapy Center. M.F. was supported by a fellowship from the German Research Foundation (#1655/1-1). S.E.B. was supported by NIH training grant 2T32 CA113263-06A1. This project has used the University of Pittsburgh shared facilities (animal facility, Genomics Research Core, Flow Cytometry) that are supported in part by the NIH award P30CA047904.

REFERENCES

1. Spitzer, M.H., Carmi, Y., Reticker-Flynn, N.E., Kwek, S.S., Madhireddy, D., Martins, M.M., Gheradini, P.F., Prestwood, T.R., Chabon, J., Bendall, S.C., et al. (2017). Systemic immunity is required for effective cancer immunotherapy. Cell *168*, 487–502.e415.
2. Gajewski, T.F., Schreiber, H., and Fu, Y.X. (2013). Innate and adaptive immune cells in the tumor microenvironment. Nat. Immunol. *14*, 1014–1022.
3. Nagarsheth, N., Wicha, M.S., and Zou, W. (2017). Chemokines in the cancer microenvironment and their relevance in cancer immunotherapy. Nat. Rev. Immunol. *17*, 559–572.
4. Prestwich, R.J., Harrington, K.J., Pandha, H.S., Vile, R.G., Melcher, A.A., and Errington, F. (2008). Oncolytic viruses: a novel form of immunotherapy. Expert Rev. Anticancer Ther. *8*, 1581–1588.
5. Bartlett, D.L., Liu, Z., Sathaiah, M., Ravindranathan, R., Guo, Z., He, Y., and Guo, Z.S. (2013). Oncolytic viruses as therapeutic cancer vaccines. Mol. Cancer *12*, 103.
6. Guo, Z.S., Liu, Z., and Bartlett, D.L. (2014). Oncolytic immunotherapy: dying the right way is a key to eliciting potent antitumor immunity. Front. Oncol. *4*, 74.
7. Kaufman, H.L., Kohlhapp, F.J., and Zloza, A. (2015). Oncolytic viruses: a new class of immunotherapy drugs. Nat. Rev. Drug Discov. *14*, 642–662.
8. Galluzzi, L., Buqué, A., Kepp, O., Zitvogel, L., and Kroemer, G. (2017). Immunogenic cell death in cancer and infectious disease. Nat. Rev. Immunol. *17*, 97–111.
9. Zafar, S., Parviainen, S., Siurala, M., Hemminki, O., Havunen, R., Tähtinen, S., Bramante, S., Vassilev, L., Wang, H., Lieber, A., et al. (2016). Intravenously usable fully serotype 3 oncolytic adenovirus coding for CD40L as an enabler of dendritic cell therapy. OncoImmunology *6*, e1265717.
10. Zamarin, D., Holmgaard, R.B., Ricca, J., Plitt, T., Palese, P., Sharma, P., Merghoub, T., Wolchok, J.D., and Allison, J.P. (2017). Intratumoral modulation of the inducible co-stimulator ICOS by recombinant oncolytic virus promotes systemic anti-tumour immunity. Nat. Commun. *8*, 14340.
11. Liu, Z., Ravindranathan, R., Li, J., Kalinski, P., Guo, Z.S., and Bartlett, D.L. (2015). CXCL11-Armed oncolytic poxvirus elicits potent antitumor immunity and shows enhanced therapeutic efficacy. OncoImmunology *5*, e1091554.
12. Veinalde, R., Grossardt, C., Hartmann, L., Bourgeois-Daigneault, M.C., Bell, J.C., Jäger, D., von Kalle, C., Ungerechts, G., and Engeland, C.E. (2017). Oncolytic measles virus encoding interleukin-12 mediates potent antitumor effects through T cell activation. OncoImmunology *6*, e1285992.
13. Alkayyal, A.A., Tai, L.H., Kennedy, M.A., de Souza, C.T., Zhang, J., Lefebvre, C., Sahi, S., Ananth, A.A., Mahmoud, A.B., Makrigiannis, A.P., et al. (2017). NK-cell recruitment Is necessary for eradication of peritoneal carcinomatosis with an IL12-expressing maraba virus cellular vaccine. Cancer Immunol. Res. *5*, 211–221.
14. Zamarin, D., Holmgaard, R.B., Subudhi, S.K., Park, J.S., Mansour, M., Palese, P., Merghoub, T., Wolchok, J.D., and Allison, J.P. (2014). Localized oncolytic virotherapy overcomes systemic tumor resistance to immune checkpoint blockade immunotherapy. Sci. Transl. Med. *6*, 226ra32.
15. Liu, Z., Ravindranathan, R., Kalinski, P., Guo, Z.S., and Bartlett, D.L. (2017). Rational combination of oncolytic vaccinia virus and PD-L1 blockade works synergistically to enhance therapeutic efficacy. Nat. Commun. *8*, 14754.
16. Lichty, B.D., Breitbach, C.J., Stojdl, D.F., and Bell, J.C. (2014). Going viral with cancer immunotherapy. Nat. Rev. Cancer *14*, 559–567.
17. Budagian, V., Bulanova, E., Paus, R., and Bulfone-Paus, S. (2006). IL-15/IL-15 receptor biology: a guided tour through an expanding universe. Cytokine Growth Factor Rev. *17*, 259–280.
18. Anguille, S., Lion, E., Tel, J., de Vries, I.J., Couderé, K., Fromm, P.D., Van Tendeloo, V.F., Smits, E.L., and Berneman, Z.N. (2012). Interleukin-15-induced CD56(+) myeloid dendritic cells combine potent tumor antigen presentation with direct tumoricidal potential. PLoS ONE *7*, e51851.
19. Zhang, X., Sun, S., Hwang, I., Tough, D.F., and Sprent, J. (1998). Potent and selective stimulation of memory-phenotype CD8+ T cells in vivo by IL-15. Immunity *8*, 591–599.
20. Kim, P.S., Kwilas, A.R., Xu, W., Alter, S., Jeng, E.K., Wong, H.C., Schlom, J., and Hodge, J.W. (2016). IL-15 superagonist/IL-15RαSushi-Fc fusion complex (IL-15SA/IL-15RαSu-Fc; ALT-803) markedly enhances specific subpopulations of NK and memory CD8+ T cells, and mediates potent anti-tumor activity against murine breast and colon carcinomas. Oncotarget *7*, 16130–16145.
21. Waldmann, T.A. (2015). The shared and contrasting roles of IL2 and IL-15 in the life and death of normal and neoplastic lymphocytes: implications for cancer therapy. Cancer Immunol. Res. *3*, 219–227.
22. Liu, R.B., Engels, B., Schreiber, K., Ciszewski, C., Schietinger, A., Schreiber, H., and Jabri, B. (2013). IL-15 in tumor microenvironment causes rejection of large established tumors by T cells in a noncognate T cell receptor-dependent manner. Proc. Natl. Acad. Sci. USA *110*, 8158–8163.
23. Dubois, S., Mariner, J., Waldmann, T.A., and Tagaya, Y. (2002). IL-15Ralpha recycles and presents IL-15 In trans to neighboring cells. Immunity *17*, 537–547.
24. Van den Bergh, J.M., Lion, E., Van Tendeloo, V.F., and Smits, E.L. (2017). IL-15 receptor alpha as the magic wand to boost the success of IL-15 antitumor therapies: The upswing of IL-15 transpresentation. Pharmacol. Ther. *170*, 73–79.
25. Wu, J. (2013). IL-15 agonists: The cancer cure cytokine. J. Mol. Genet. Med. *7*, 85.
26. Stoklasek, T.A., Schluns, K.S., and Lefrançois, L. (2006). Combined IL-15/IL-15Ralpha immunotherapy maximizes IL-15 activity in vivo. J. Immunol. *177*, 6072–6080.
27. Dubois, S., Patel, H.J., Zhang, M., Waldmann, T.A., and Müller, J.R. (2008). Preassociation of IL-15 with IL-15R alpha-IgG1-Fc enhances its activity on proliferation of NK and CD8+/CD44high T cells and its antitumor action. J. Immunol. *180*, 2099–2106.
28. Epardaud, M., Elpek, K.G., Rubinstein, M.P., Yonekura, A.R., Bellemare-Pelletier, A., Bronson, R., Hamerman, J.A., Goldrath, A.W., and Turley, S.J. (2008). Interleukin-15/interleukin-15R alpha complexes promote destruction of established tumors by reviving tumor-resident CD8+ T cells. Cancer Res. *68*, 2972–2983.
29. Rhode, P.R., Egan, J.O., Xu, W., Hong, H., Webb, G.M., Chen, X., Liu, B., Zhu, X., Wen, J., You, L., et al. (2016). Comparison of the superagonist complex, ALT-803, to IL-15 as cancer immunotherapeutics in animal models. Cancer Immunol. Res. *4*, 49–60.
30. Desbois, M., Le Vu, P., Coutzac, C., Marcheteau, E., Béal, C., Terme, M., Gey, A., Morisseau, S., Teppaz, G., Boselli, L., et al. (2016). IL-15 trans-signaling with the superagonist RLI promotes effector/memory CD8+ T cell responses and enhances antitumor activity of PD-1 antagonists. J. Immunol. *197*, 168–178.
31. Stephenson, K.B., Barra, N.G., Davies, E., Ashkar, A.A., and Lichty, B.D. (2012). Expressing human interleukin-15 from oncolytic vesicular stomatitis virus improves survival in a murine metastatic colon adenocarcinoma model through the enhancement of anti-tumor immunity. Cancer Gene Ther. *19*, 238–246.
32. Nishio, N., Diaconu, I., Liu, H., Cerullo, V., Caruana, I., Hoyos, V., Bouchier-Hayes, L., Savoldo, B., and Dotti, G. (2014). Armed oncolytic virus enhances immune functions of chimeric antigen receptor-modified T cells in solid tumors. Cancer Res. *74*, 5195–5205.
33. Tosic, V., Thomas, D.L., Kranz, D.M., Liu, J., McFadden, G., Shisler, J.L., MacNeill, A.L., and Roy, E.J. (2014). Myxoma virus expressing a fusion protein of interleukin-15 (IL-15) and IL-15 receptor alpha has enhanced antitumor activity. PLoS ONE *9*, e109801.
34. Chan, W.M., and McFadden, G. (2014). Oncolytic poxviruses. Annu. Rev. Virol. *1*, 119–141.
35. McCart, J.A., Ward, J.M., Lee, J., Hu, Y., Alexander, H.R., Libutti, S.K., Moss, B., and Bartlett, D.L. (2001). Systemic cancer therapy with a tumor-selective vaccinia virus mutant lacking thymidine kinase and vaccinia growth factor genes. Cancer Res. *61*, 8751–8757.
36. Zeh, H.J., Downs-Canner, S., McCart, J.A., Guo, Z.S., Rao, U.N., Ramalingam, L., Thorne, S.H., Jones, H.L., Kalinski, P., Wieckowski, E., et al. (2015). First-in-man study of western reserve strain oncolytic vaccinia virus: safety, systemic spread, and antitumor activity. Mol. Ther. *23*, 202–214.
37. Downs-Canner, S., Guo, Z.S., Ravindranathan, R., Breitbach, C.J., O'Malley, M.E., Jones, H.L., Moon, A., McCart, J.A., Shuai, Y., Zeh, H.J., and Bartlett, D.L. (2016). Phase 1 study of intravenous oncolytic poxvirus (vvDD) in patients with advanced solid cancers. Mol. Ther. *24*, 1492–1501.
38. Kinter, A.L., Godbout, E.J., McNally, J.P., Sereti, I., Roby, G.A., O'Shea, M.A., and Fauci, A.S. (2008). The common gamma-chain cytokines IL-2, IL-7, IL-15, and

IL-21 induce the expression of programmed death-1 and its ligands. J. Immunol. *181*, 6738–6746.

39. Kirwan, S., Merriam, D., Barsby, N., McKinnon, A., and Burshtyn, D.N. (2006). Vaccinia virus modulation of natural killer cell function by direct infection. Virology *347*, 75–87.

40. Di Pilato, M., Mejías-Pérez, E., Sorzano, C.O.S., and Esteban, M. (2017). Distinct Roles of Vaccinia Virus NF-κB Inhibitor Proteins A52, B15, and K7 in the Immune Response. J. Virol. *91*, e00575-17.

41. Ren, H., Ferguson, B.J., Maluquer de Motes, C., Sumner, R.P., Harman, L.E., and Smith, G.L. (2015). Enhancement of CD8(+) T-cell memory by removal of a vaccinia virus nuclear factor-κB inhibitor. Immunology *145*, 34–49.

42. Guo, Z.S., Liu, Z., Kowalsky, S., Feist, M., Kalinski, P., Lu, B., Storkus, W.J., and Bartlett, D.L. (2017). Oncolytic immunotherapy: Conceptual evolution, current strategies, and future perspectives. Front. Immunol. *8*, 555.

43. Yan, X., Wang, L., Zhang, R., Pu, X., Wu, S., Yu, L., Meraz, I.M., Zhang, X., Wang, J.F., Gibbons, D.L., et al. (2017). Overcoming resistance to anti-PD immunotherapy in a syngeneic mouse lung cancer model using locoregional virotherapy. OncoImmunology *7*, e1376156.

44. Ribas, A., Dummer, R., Puzanov, I., VanderWalde, A., Andtbacka, R.H.I., Michielin, O., Olszanski, A.J., Malvehy, J., Cebon, J., Fernandez, E., et al. (2017). Oncolytic virotherapy promotes intratumoral T cell infiltration and improves anti-PD-1 immunotherapy. Cell *170*, 1109–1119.e1110.

45. Chesney, J., Puzanov, I., Collichio, F., Singh, P., Milhem, M.M., Glaspy, J., Hamid, O., Ross, M., Friedlander, P., Garbe, C., et al. (2018). Randomized, Open-Label Phase II Study Evaluating the Efficacy and Safety of Talimogene Laherparepvec in Combination With Ipilimumab Versus Ipilimumab Alone in Patients With Advanced, Unresectable Melanoma. J. Clin. Oncol. *36*, 1658–1667.

46. Guo, Z.S., Parimi, V., O'Malley, M.E., Thirunavukarasu, P., Sathaiah, M., Austin, F., and Bartlett, D.L. (2010). The combination of immunosuppression and carrier cells significantly enhances the efficacy of oncolytic poxvirus in the pre-immunized host. Gene Ther. *17*, 1465–1475.

47. Obermajer, N., Urban, J., Wieckowski, E., Muthuswamy, R., Ravindranathan, R., Bartlett, D.L., and Kalinski, P. (2018). Promoting the accumulation of tumor-specific T cells in tumor tissues by dendritic cell vaccines and chemokine-modulating agents. Nat. Protoc. *13*, 335–357.

48. Rintoul, J.L., Wang, J., Gammon, D.B., van Buuren, N.J., Garson, K., Jardine, K., Barry, M., Evans, D.H., and Bell, J.C. (2011). A selectable and excisable marker system for the rapid creation of recombinant poxviruses. PLoS ONE *6*, e24643.

49. Guo, Z.S., Liu, Z., Sathaiah, M., Wang, J., Ravindranathan, R., Kim, E., Huang, S., Kenniston, T.W., Bell, J.C., Zeh, H.J., 3rd, et al. (2017). Rapid generation of multiple loci-engineered marker-free poxvirus and characterization of a clinical-grade oncolytic vaccinia virus. Mol. Ther. Methods Clin. Dev. *7*, 112–122.

50. Zinn, K.R., Chaudhuri, T.R., Szafran, A.A., O'Quinn, D., Weaver, C., Dugger, K., Lamar, D., Kesterson, R.A., Wang, X., and Frank, S.J. (2008). Noninvasive bioluminescence imaging in small animals. ILAR J. *49*, 103–115.

YMTHE, Volume *26*

Supplemental Information

Superagonist IL-15-Armed Oncolytic Virus Elicits Potent Antitumor Immunity and Therapy That Are Enhanced with PD-1 Blockade

Stacy J. Kowalsky, Zuqiang Liu, Mathilde Feist, Sara E. Berkey, Congrong Ma, Roshni Ravindranathan, Enyong Dai, Edward J. Roy, Zong Sheng Guo, and David L. Bartlett

Supplemental Figure 1. The cytotoxicity of oncolytic viruses in MC38 colon cancer cells

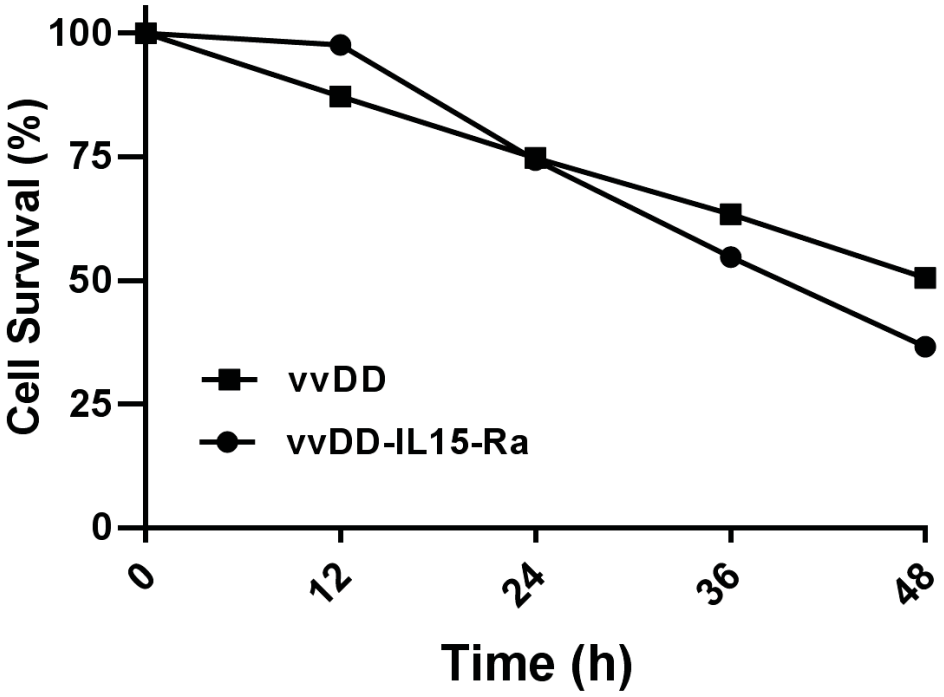

Supplemental Figure 2. PD-1 and PD-L1 expression (RT-qPCR)

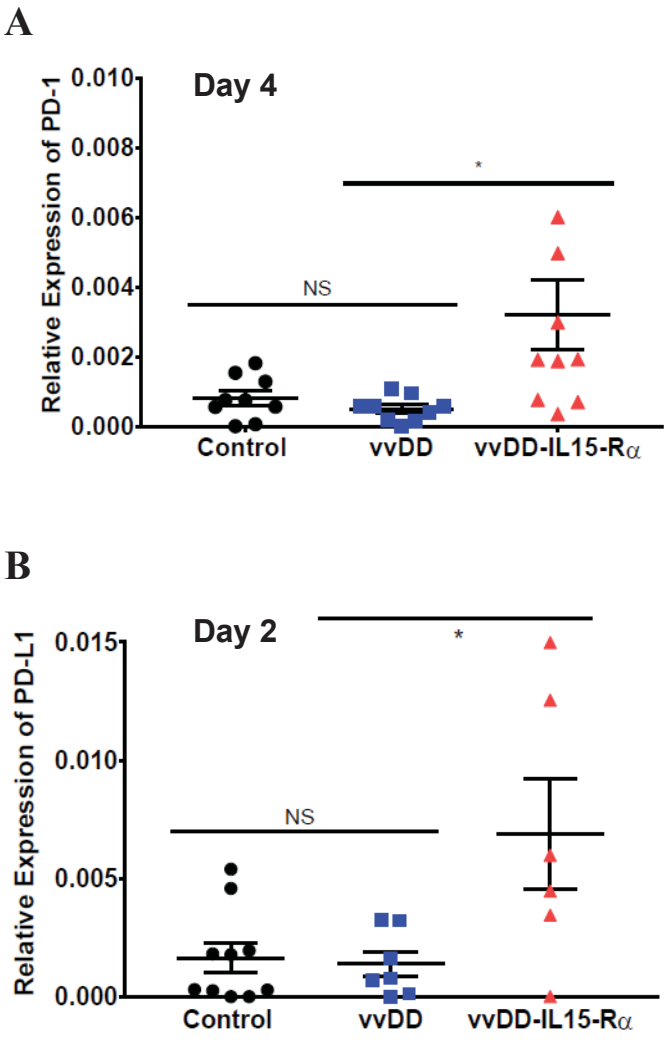

Supplemental Table 1. Viral therapeutic and survival data by experimental model

§ Survival data not represented graphically

Experiment	Treatment Group	n	Median survival (days)	*p* vs Control	*p* vs vvDD	*p* vs vvDD-IL15-Rα
MC38 Tumor Progression/ Survival (Fig. 3)	Control	9	18	-	***	***
	vvDD	8	36	***	-	***
	vvDD-IL15-Rα	5	> 130	***	***	-
ID8 Tumor Progression/ Survival (Fig. 4)	Control	10	46.5	-	****	****
	vvDD	9	87	****	-	*
	vvDD-IL15-Rα	10	> 130	****	*	-

Experiment	Treatment Group	n	Median survival (days)	*p* vs Control	*p* vs vvDD-IL15-Rα	*p* vs Virus + α-CD8	*p* vs Virus + α-NK cell	*p* vs Virus + α-CD4
Selective Immune Depletion (Fig. 5E,F) §	Control	9	18	-	****	****	****	****
	vvDD-IL15-Rα	10	> 150	****	-	**	NS	NS
	Virus + α-CD8	10	51.5	****	**	-	**	***
	Virus + α-NK cell	10	> 150	****	NS	**	-	NS
	Virus + α-CD4	10	> 150	****	NS	***	NS	-

Experiment	Treatment Group	n	Median survival (days)	*p* vs Control	*p* vs α-PD1	*p* vs vvDD	*p* vs vvDD-IL15-Rα	*p* vs vvDD+ α-PD1	*p* vs vvDD-IL15-Rα+ α-PD-1
Combination with PD-1 Blockade (Fig. 6B)	Control	7	20	-	*	***	***	***	***
	α-PD1	7	27	*	-	NS	***	**	***
	vvDD	7	31	***	NS	-	**	*	***
	vvDD-IL15-Rα	8	40	***	***	**	-	NS	***
	vvDD + α-PD1	8	38.5	***	**	*	NS	-	***
	vvDD-IL15-Rα + α-PD1	7	> 200	***	***	***	***	***	-

Supplemental Table 2. RT-qPCR Primers Utilized

Primer	Thermo Fisher Scientific primer	Gene symbol	RefSeq	Translated Protein	
CD8	Mm01182107_g1	CD8a	NM_001081110.2 NM_009857.1	NP_001074579.1 NP_033987.1	
NKp46	Mm00456776_g1	Ncr1	NM_010746.3	NP_034876.2	
NKG2D	Mm00473603_m1	Klrk1	NM_001083322.2 NM_001286018.1 NM_033078.4	NP_001076791.1 NP_001272947.1 NP_149069.1	
PD-1	Mm1285676_m1	Pdcd1	NM_008798.2	NP_03824.1	
PDL-1	Mm00452054_m1	CD274	NM_021893.3	NP_068693.1	
HPRT¶	Mm00446968_m1	Hprt	NM_0135562.2	NP_038584.2	
GAPDH¶	Mm99999915_g1	Gapdh	NM_00128926.1 NM_008084.3	NP_001276655.1 NP_032110.1	
Custom Primer			**Forward Sequence**	**Reverse Sequence**	**Reporter sequence**
A34R	-	-	GTCTACAGATAATGCGGTTTATCAGTGT	ACTCTCAGATGTCTAGTATCCGGTCTA	CTGGCTCGTAATTTAC
			Forward Sequence	**Reverse Sequence**	**Hybridization Oligomer**
IL15-Rα	-	-	TGAGGAACGTGCTGTACCTG	GGTCTTCTCCTCCAGCTCCT	GAGAGCGGCTGTAAGGAGTG

1. ¶ house-keeping genes.